

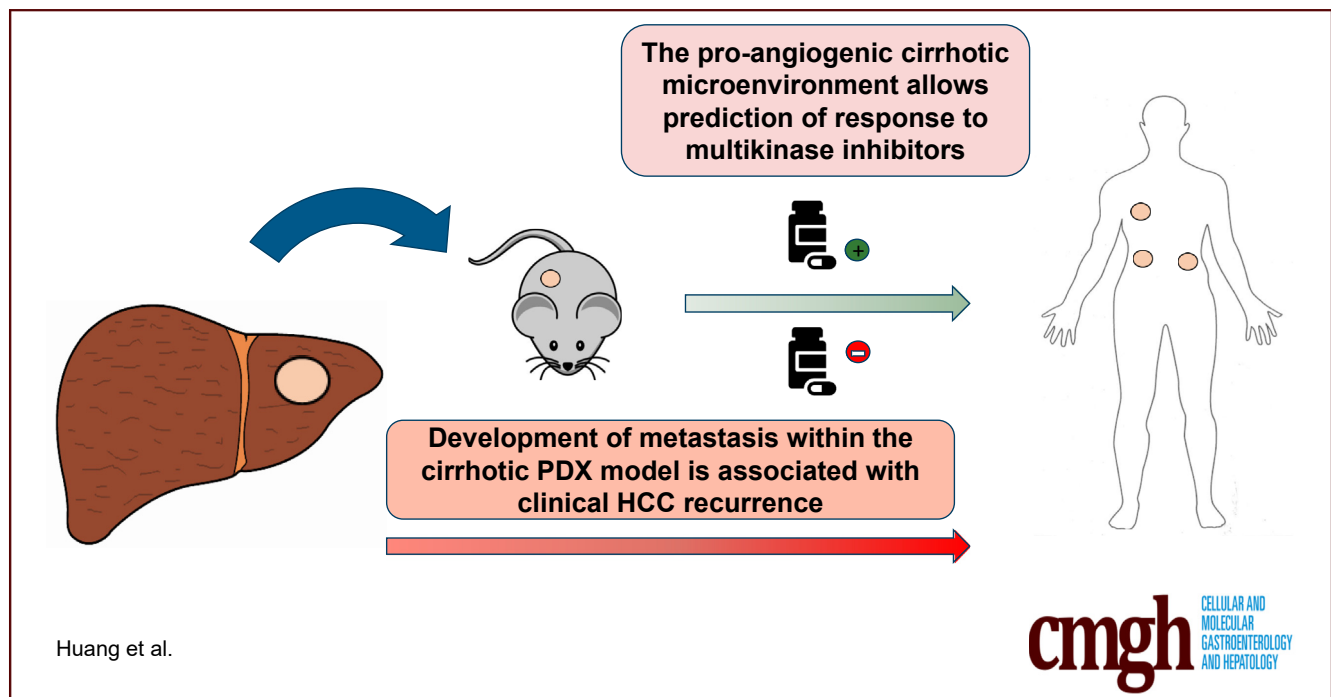
ORIGINAL RESEARCH

Predicting HCC Response to Multikinase Inhibitors With In Vivo Cirrhotic Mouse Model for Personalized Therapy



Daniel Q. Huang,^{1,2} Mark D. Muthiah,^{1,2} Lei Zhou,² Halisah Jumat,² Wan Xin Tan,² Guan Huei Lee,^{1,2} Seng Gee Lim,^{1,2} Alfred Kow,³ Glenn Bonney,³ Iyer Shridhar,³ Yi Ting Lim,⁴ Aileen Wee,⁵ Yin Huei Pang,⁶ Gwyneth Soon,⁶ Pierce Chow,^{7,8,9} and Yock Young Dan^{1,2}

¹Division of Gastroenterology and Hepatology, Department of Medicine, National University Health System, Singapore; ²Department of Medicine, Yong Loo Lin School of Medicine, National University of Singapore, Singapore; ³Division of Hepatobiliary and Pancreatic Surgery, Department of Surgery, National University Health System, Singapore; ⁴Department of Diagnostic Imaging, National University Health System, Singapore; ⁵Department of Pathology, Yong Loo Lin School of Medicine, National University of Singapore, National University Hospital, National University Health System, Singapore; ⁶Department of Pathology, National University Hospital, National University Health System, Singapore; ⁷Division of Surgical Oncology, National Cancer Center Singapore, Singapore; ⁸Department of Hepato-Pancreato-Biliary and Transplant Surgery, Singapore General Hospital, Singapore; and ⁹Duke-NUS Medical School Singapore, Singapore



SUMMARY

The cirrhotic microenvironment that surrounds hepatocellular carcinoma promotes growth of new blood vessels. Current patient-derived animal models are noncirrhotic and they are unable to accurately evaluate the effect of multikinase inhibitors, which act by reducing tumor blood supply. We present a novel cirrhotic mouse model that predicts the natural biology of hepatocellular carcinoma and allows personalized therapy.

BACKGROUND & AIMS: Hepatocellular carcinoma (HCC) arises in a cirrhotic, pro-angiogenic microenvironment. Inhibiting angiogenesis is a key mode of action of multikinase inhibitors and current non-cirrhotic models are unable to predict treatment response. We present a novel mouse cirrhotic model of xenotransplant that predicts the natural biology of HCC and allows personalized therapy.

METHODS: Cirrhosis was induced in NOD Scid gamma mice with 4 months of thioacetamide administration. Patient derived xenografts (PDXs) were created by transplant of human HCC

subcutaneously into non-cirrhotic mice and intra-hepatically into both cirrhotic and non-cirrhotic mice. The applicability of cirrhotic PDXs for drug testing was tested with 16 days of either sorafenib or lenvatinib. Treatment response was evaluated by MRI.

RESULTS: 8 out of 19 (42%) human HCC engrafted in the cirrhotic model compared with only 3 out of 19 (16%) that engrafted in the subcutaneous non-cirrhotic model. Tumor vasculature was preserved in the cirrhotic model but was diminished in the non-cirrhotic models. Metastasis developed in 3 cirrhotic PDX lines and was associated with early HCC recurrence in all 3 corresponding patients (100%), compared with only 5 out of 16 (31%) of the other PDX lines, $P = .027$. The cirrhotic model was able to predict response and non-response to lenvatinib and sorafenib respectively in the corresponding patients. Response to lenvatinib in the cirrhotic PDX was associated with reduction in CD34, VEGFR2 and CLEC4G immunofluorescence area and intensity (all $P \leq .03$).

CONCLUSIONS: A clinically relevant cirrhotic PDX model preserves tumor angiogenesis and allows prediction of response to multikinase inhibitors for personalized therapy. (*Cell Mol Gastroenterol Hepatol* 2021;11:1313–1325; <https://doi.org/10.1016/j.jcmgh.2020.12.009>)

Keywords: Xenograft; Hepatocellular Carcinoma; Multikinase Inhibitors.

Most (80%–90%) hepatocellular carcinoma (HCC) occurs in cirrhotic livers.^{1,2} Unlike clonal homogeneous tumors, HCC pathophysiology is complex, involving a combination of transformed hepatocytic epithelial cells, oncogenic endothelial angiogenic cells, and permissive supportive stromal and immune cells operating under the proinflammatory and profibrotic milieu of a cirrhotic liver. The inflammatory chemokines, cell death signals, extracellular matrix, and regenerative growth signals constitute a perfect storm for hepatocarcinogenesis to occur.³ This tumor-cirrhotic microenvironmental interaction in defining the biology of the HCC is still poorly understood because traditional patient-derived cancer cell lines or simple subcutaneous or intrahepatic xenografts are inadequate in recapitulating the cirrhotic microenvironment from which HCC arises.⁴

In cirrhosis, the excess fibrotic extracellular matrix surrounding HCC results in altered blood flow and hypoxia, resulting in upregulation of growth factors, cytokines, and metalloproteinases, inducing angiogenesis.^{5,6} Activated hepatic stellate cells in cirrhotic livers further promote angiogenesis and micrometastases by releasing vascular endothelial growth factor.⁷ Tumor angiogenesis assessed by anti-CD34 has been shown to be associated with poor prognosis in patients with HCC but also predictive of response to sorafenib.^{8,9} Sorafenib and lenvatinib inhibit multiple kinases involved in angiogenesis and have shown benefit in the treatment of HCC, although objective response rates are less than 25%.^{10,11} Despite more than 10 years of experience with sorafenib, there is neither a good clinical biomarker nor a preclinical model that predicts response to

multikinase inhibitors, resulting in less than a quarter of patients responding to systemic therapy.^{12–14}


HCC represents an unhappy combination of 2 diseases: tumor and liver cirrhosis. Existing noncirrhotic patient-derived xenograft (PDX) models only account for the tumor component but omit cirrhosis, a key determinant of outcomes.^{15,16} Several groups have attempted to use HCC PDXs to predict response to multikinase inhibitors without success, possibly because they lack the cirrhotic proangiogenic microenvironment necessary to replicate the key mode of action of these agents.^{13,14,17} There is an unmet need for a clinically relevant animal model that simulates the natural biology of HCC to allow for more accurate prediction of tumor response to multikinase inhibitors. Using thioacetamide-induced cirrhosis,¹⁸ we report a novel mouse cirrhotic model of xenotransplant that allows in vivo testing of response to multikinase inhibitor therapy and targeted therapy.

Results

Cirrhotic Patient-Derived Xenograft

Nineteen consecutive HCC specimens in cirrhotic livers were used for transplantation intrahepatically into chemically induced cirrhotic livers (Figure 1). Sixteen of the 19 (84.2%) individuals were male, with a median age of 53.5 (44.0–62.0) years (Table 1). All individuals had cirrhosis and were Child-Pugh A. Eight out of 19 (42.1%) successfully engrafted in xenografts that could be serially maintained for more than 5 generations over 6 months. There was a higher proportion of poorly differentiated histology among human HCC that engrafted into the cirrhotic model versus HCC that did not engraft (87.5% [7 out of 8] vs 18.2% [2 out of 11]; $P = .003$) (Table 1). In comparison, the HCC that did not engraft into the cirrhotic model had a higher proportion of moderately differentiated histology (72.7% [8 out of 11] vs 12.5% [1 out of 8]; $P = .009$) compared with HCC that engrafted. Only 1 of the HCC that did not engraft into the cirrhotic model was well differentiated, compared with none in the HCC that engrafted. The engrafted tumors showed thick trabeculae with marked nuclear pleomorphism and paucity of albumin, α -fetoprotein, or EPCAM staining; instead they showed colabelling of both the mesenchymal marker vimentin and the epithelial marker E cadherin within the same cells in 6 out of 8 tumors and staining for vascular endothelial growth factor receptor 2 (VEGFR2) in 3 out of 8 tumors. In comparison, the non-engrafted tumors did not display similar colabelling of vimentin and E cadherin and were negative for VEGFR2. The engrafted tumors showed similar morphologic features to

Abbreviations used in this paper: CLEC4G, C-type lectin superfamily 4 member G; HCC, hepatocellular carcinoma; MRI, magnetic resonance imaging; NSG, NOD Scid Gamma; PDX, patient-derived xenograft; VEGFR, vascular endothelial growth factor receptor 2.

 Most current article

© 2021 The Authors. Published by Elsevier Inc. on behalf of the AGA Institute. This is an open access article under the CC BY-NC-ND license (<http://creativecommons.org/licenses/by-nc-nd/4.0/>).

2352-345X

<https://doi.org/10.1016/j.jcmgh.2020.12.009>

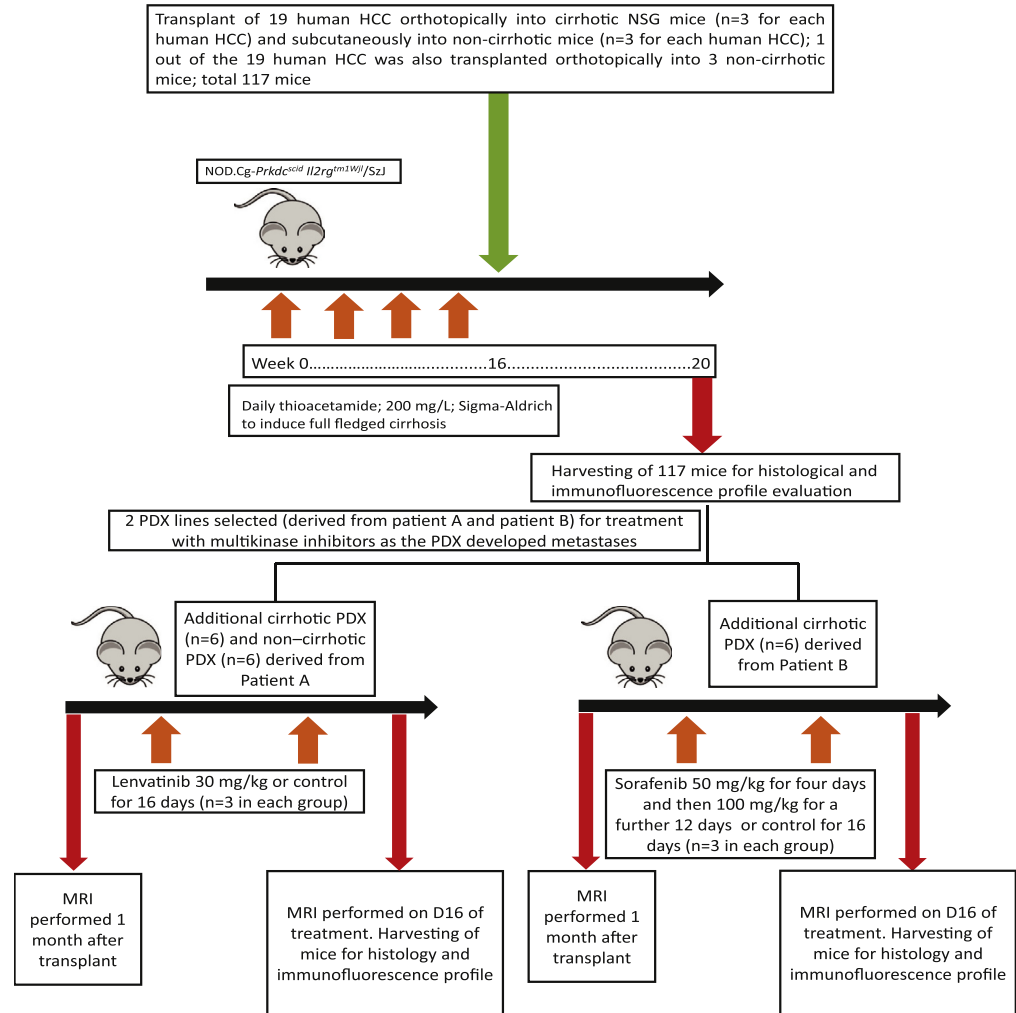


Figure 1. Flowchart of the cirrhotic patient-derived xenograft program.

the human tumor tissue, comprising markedly thickened trabeculae and solid nests of cells with conspicuous nuclear pleomorphism, occasional multinucleation, and frequent bizarre mitoses (Figure 2A).

Metastasis in the Cirrhotic Xenograft Was Associated With Hepatocellular Carcinoma Recurrence

Of the 8 human HCC that engrafted into the cirrhotic PDX, 3 of the poorly differentiated engrafted HCC developed pulmonary metastasis in the cirrhotic PDX (Figure 2B). Metastasis in the cirrhotic PDXs was associated with early clinical recurrence in all 3 corresponding patients (100%). In comparison, in the absence of metastasis or engraftment in the cirrhotic PDX, only 5 out of 16 (31.2%) corresponding patients developed clinical recurrence ($P = .027$).

Noncirrhotic Xenograft: Subcutaneous and Orthotopic

Three out of 19 (15.8%) HCCs engrafted into the subcutaneous, noncirrhotic model. These were all poorly

differentiated and only 1 patient developed clinical recurrence. The engrafted tumors in the subcutaneous noncirrhotic xenograft model appeared sarcomatoid and even more poorly differentiated compared with the human HCC tissue, with a more solid appearance and loss of the sinusoidal-trabecular architecture (Figure 2A). None of the engrafted subcutaneous PDX models developed metastasis.

To test the criticality of cirrhosis on xenograft HCC biology, we selected a single PDX line (derived from 1 of the 19 patients with HCC) that developed metastasis in the cirrhotic PDX model. We transplanted this human HCC PDX line intrahepatically into 3 noncirrhotic NOD Scid Gamma (NSG) mice. The tumors in the noncirrhotic orthotopic xenograft model displayed a sarcomatoid appearance with vague fascicles of somewhat spindled cells, differing in appearance to the human HCC tissue that was used for implantation (Figure 2A). Although the same PDX line was transplanted into the orthotopic noncirrhotic PDX model and the cirrhotic PDX model, 2 out of 3 cirrhotic PDX mice developed metastasis, whereas none of the orthotopic noncirrhotic mice developed metastasis.

Table 1. Clinicopathologic Features of Patients With HCC

Patient demographics and tumor characteristics	Patients (N = 19)
Age, median (IQR)	53.5 (44.0–62.0)
Male/female, n	16/3
HBV/NASH/HCV/alcohol	10/5/3/1
Child Pugh Score, A/B/C	19/0/0
MELD, median (IQR)	7 (7–9)
AFP, median (IQR), ng/mL	25.0 (6.0–639.0)
Tumor total diameter, >5/<5 (cm), n	14/5
Vascular invasion, n	9
BCLC stage, 0 or A/B or C, n	10/9
Tumor grade among engrafted human HCC: well differentiated, moderately differentiated, poorly differentiated, n	0/1/7
Tumor grade among nonengrafted human HCC: well differentiated, moderately differentiated, poorly differentiated, n	1/8/2

AFP, α -fetoprotein; BCLC, Barcelona Clinic Liver Cancer staging; HBV, hepatitis B virus; HCC, hepatocellular carcinoma; HCV, hepatitis C; IQR, interquartile range; MELD, model for end-stage liver disease; NASH, nonalcoholic steatohepatitis.

Preservation of Tumor Vasculature in Cirrhotic, But Not Noncirrhotic Xenograft

To evaluate tumor angiogenesis within the xenograft models, the same PDX line (derived from 1 of the 19 patients with HCC) was transplanted into the cirrhosis and noncirrhosis models, and tumor vasculature was assessed by CD34 antibody fluorescence. Tumor vasculature was preserved in the cirrhotic PDX model, but the noncirrhotic models (subcutaneous and orthotopic) were almost avascular (Figure 2C). CD34 immunofluorescence was similar between the human HCC and the cirrhotic PDX by both intensity ($P = .24$) and area ($P = .54$) quantification (Figure 2D). However, when compared with human HCC, CD34 immunofluorescence was diminished in the orthotopic and subcutaneous noncirrhotic models by intensity (both $P < .001$) and area (both $P < .01$) (Figure 2D). Of note, mouse-specific but not human-specific CD34 and VEGFR2 antibody fluorescence was present in the cirrhotic PDX model, suggesting that the murine endothelial cells contributed to ingrowth of blood vessels to support tumor growth.

The Cirrhotic Xenograft Model Predicted Clinical Response to Lenvatinib

To evaluate if the cirrhotic PDX model could predict response to multikinase inhibitors, we treated 3 cirrhotic PDX derived from a patient with hepatitis C cirrhosis and HCC (Patient A) with lenvatinib and compared this against

treatment of 3 cirrhotic PDX with control (Figure 1). We selected this xenograft line because the cirrhotic PDX line had developed lung metastases and the patient had also developed clinical HCC recurrence. Magnetic resonance imaging (MRI) after 16 days of treatment showed a decrease in mean tumor volume in the lenvatinib group versus an increase in mean tumor volume of the control group (-12.06 mm^3 vs 485.3 mm^3 ; $P = .031$), respectively (Figure 3A). The waterfall plot for change in tumor volume (%) is shown in Figure 3B.

To demonstrate the criticality of the cirrhotic microenvironment in prediction of clinical response to lenvatinib, we treated 3 noncirrhotic PDX derived from the same patient with hepatitis C cirrhosis and HCC (Patient A) with lenvatinib; we then compared this against treatment of 3 noncirrhotic orthotopic PDX with control. MRI after 16 days of treatment showed an increase in mean tumor volume in both the lenvatinib group and control group (162.11 mm^3 vs 84.12 mm^3 ; $P = .21$), respectively (Figure 3C and D).

Response to lenvatinib in the cirrhotic xenograft correlated with clinical response to lenvatinib in Patient A. A repeat MRI 2 months after initiation of lenvatinib demonstrated partial response according to modified Response Evaluation Criteria in Solid Tumors (mRECIST) (Figure 3E).

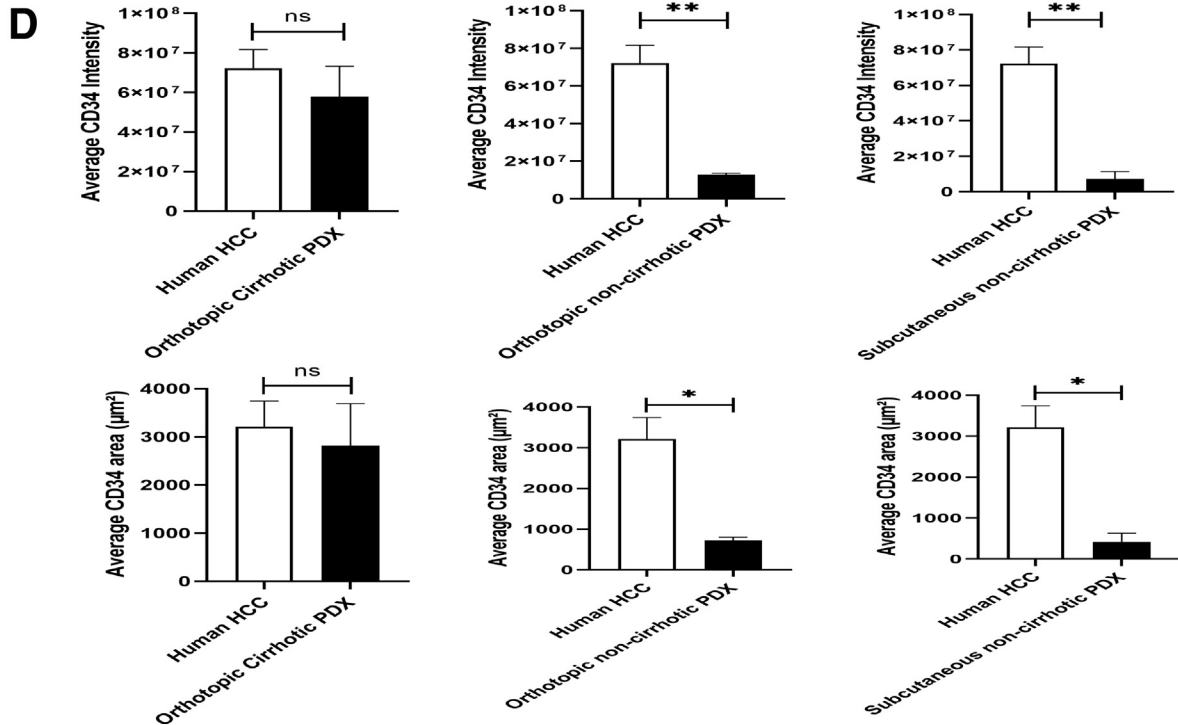
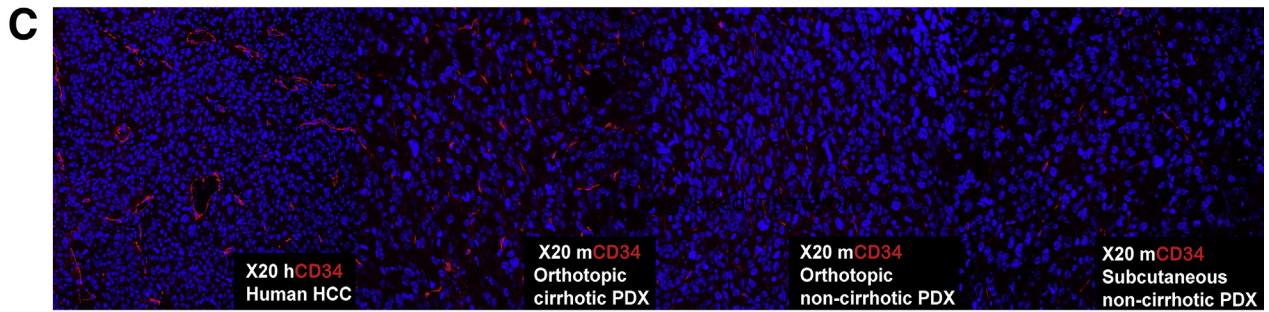
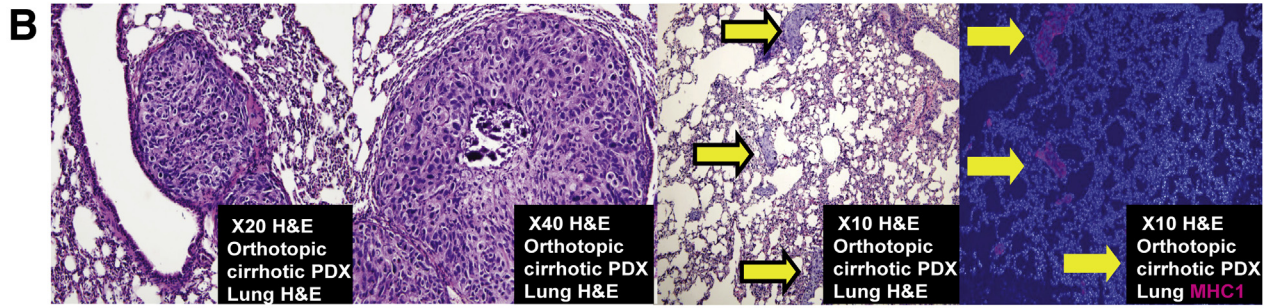
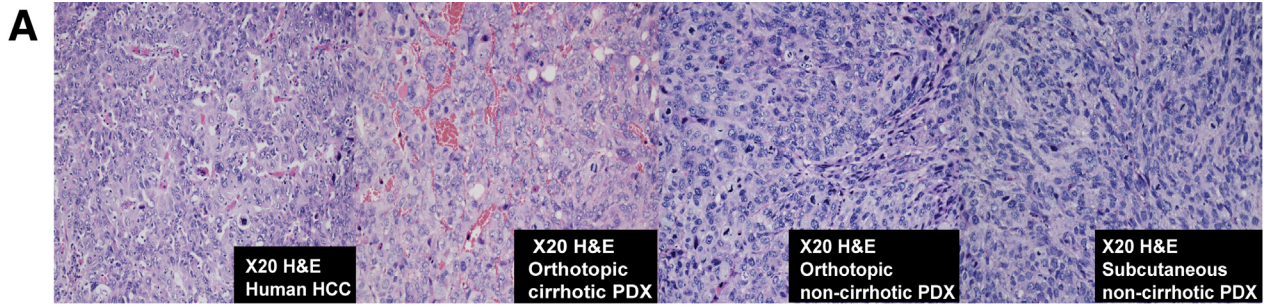
The Cirrhotic Xenograft Model Predicted Nonresponse to Sorafenib

We selected a second PDX line derived from a patient with hepatitis B cirrhosis (Patient B) because the PDX model had also developed metastases. Three cirrhotic PDX derived from Patient B were treated with sorafenib and compared against treatment of 3 cirrhotic PDX with control (Figure 1). MRI done 16 days apart showed no significant difference in tumor volume changes between sorafenib and control arms (an increase of 88.68 mm^3 vs 147.50 mm^3 , respectively; $P = .59$) (Figure 4A). The waterfall plot for change in tumor volume (%) is shown in Figure 4B.

Patient B developed early HCC recurrence postsurgery with metastases in the liver and lung. A computed tomography scan 2 months after Patient B started sorafenib revealed progressive disease with enlargement of the HCC and extrahepatic metastases, correlating with poor response to sorafenib in the cirrhotic model (Figure 4C).

Response to Multikinase Inhibitor Is Associated With Diminished Tumor Vasculature

Administration of lenvatinib to the cirrhotic xenograft established from Patient A resulted in reduced CD34, VEGFR2, and C-type lectin superfamily 4 member G (CLEC4G; Abcam, Cambridge, UK) antibody fluorescence by both intensity ($P = .002$, $P = .001$, and $P = .03$, respectively) and area ($P = .0008$, $P = .002$, and $P = .02$, respectively) when compared with administration of control (Figure 5). There was no significant change in CD34, VEGFR2, and CLEC4G antibody immunofluorescence by intensity or area after administration of sorafenib to the cirrhotic xenograft established from Patient B, all $P > .30$ (Figure 5).



Discussion

Compared with other cancers, systemic therapy in HCC has modest efficacy and objective response rates of less than 30%.^{10,19} This is in part because of the heterogeneity of HCC and the intrinsic complexity of HCC pathogenesis in a microenvironment that is still poorly understood. With the technical challenges of a reliable in vitro culture system, an in vivo xenograft model represents the most practical platform for studying liver cancer biology and testing drugs for personalized therapy.²⁰ In this study, we establish a novel cirrhotic PDX model that predicts response to multikinase inhibitors by preserving tumor vasculature.

HCC typically occurs in cirrhotic livers where attempted self-regenerating hepatocytes or progenitors become transformed in a pro-inflammatory and profibrotic environment. Current animal models of genetically modified spontaneous HCC models, or chemically induced (diethylnitrosamine) models do not recapitulate this natural carcinogenesis process. Traditional xenograft models, such as the subcutaneous or intrahepatic models, also lack the cirrhotic fertile microenvironment that plays a key role in driving the HCC biology.¹⁸ The fact that until recently, only the multikinase inhibitors have been found to be efficacious in the treatment of advanced HCC, and the lack of understanding of their mechanism of action underlines the complex interplay between epithelial-stromal and vascular components within the oncogenic milieu of cirrhotic liver.^{21,22}

Neovascularization is a key feature of HCC, with VEGFR driving endothelial cell proliferation and survival.²³ Sorafenib and lenvatinib are inhibitors of VEGFR, and reduction of tumor blood supply is a key mode of action of these drugs.^{24,25} In this study, we demonstrate how the cirrhotic microenvironment is critical to neovascularization. It is not surprising that existing noncirrhotic HCC animal models have not been able to predict response to multikinase inhibitors.²⁶ In a subcutaneous PDX model with noncirrhotic NSG mice attempting to predict HCC response to sorafenib, Hu et al¹⁴ identified 2 xenografts that showed poor response to sorafenib, and the 2 corresponding patients developed progressive disease. However, the authors were not able to predict a positive response to sorafenib. Gu et al¹³ established a cohort of subcutaneous PDXs derived from patients with HCC using BALB/c athymic or SCID mice,

and described differential responses to sorafenib and lenvatinib, but similarly were not able to predict clinical response. Wu et al¹⁷ treated PDXs established in NSG mice with sorafenib, but did not correlate this with patient treatment response. In comparison, our cirrhotic PDX model was able to preserve tumor biology and predict response and nonresponse to multikinase inhibitors in humans. We note that an orthotopic mouse model of HCC with underlying cirrhosis has been previously reported by Reiberger et al²⁷; the authors in this study induced cirrhosis using carbon tetrachloride and either implanted mouse HCC cell lines or induced de novo HCC using genetically engineered mice. Our study builds on this concept by using cirrhotic PDX to predict response to multikinase inhibitors.

Interestingly, the vascular component of our xenograft seems to be mainly mouse derived rather than human HCC derived. This highlights the crucial role of the nascent liver vascular component and microenvironment in supporting HCC and predicting outcome in patients after treatment. Although no biomarkers in clinical practice have been found to predict sorafenib response, VEGFR2 levels have been reported to correlate with tumor response again highlighting the key role of the supporting vascular stroma in a cirrhotic model for testing drug efficacy.²⁸

Our engraftment rate of 40% is comparable or better than most reported studies of xenograft induction.^{17,29,30} An interesting finding was that the cirrhotic model selects aggressive HCC subtype with mesenchymal features. Although the well-differentiated HCCs are not represented in our xenografts, in real world clinical practice, the less aggressive HCCs tend to respond well to standard therapy.^{31,32} In contrast, it is precisely the aggressive HCC that are picked up by our xenotransplant models that tends to recur after surgery or transplantation and would potentially benefit from targeted therapy. Although limited by a small sample size, the presence of metastasis in our cirrhotic xenograft models correlates closely with actual clinical recurrence. Our findings warrant further studies for clinical validation. More studies are required to evaluate if post-resection patients with HCC that engraft and develop metastases in the cirrhotic model will benefit from adjuvant therapy with personalized systemic therapy.

To our knowledge, this is the first reported cirrhotic PDX model that predicts response to multikinase inhibitors.

Figure 2. (See previous page). A cirrhotic microenvironment allows better preservation of tumor characteristics and vasculature. (A) Hematoxylin and eosin of a representative human HCC that was transplanted intrahepatically into an NSG mouse with thioacetamide-induced cirrhosis; the same human HCC was also transplanted intrahepatically into an NSG mouse treated with control instead of thioacetamide, and subcutaneously into an NSG mouse treated with control. The tumor in the cirrhotic PDX model had a closer resemblance to human HCC as compared with the noncirrhotic models. (B) Hematoxylin and eosin of a representative cirrhotic PDX that developed lung metastasis. Arrows indicate lung metastases. MHC1 immunolabelling confirmed that the metastases were of human origin. The noncirrhotic subcutaneous PDX did not develop metastasis. (C) CD34 fluorescence was demonstrated in the original human HCC. After transplantation of the same human HCC into the cirrhotic model and the 2 noncirrhotic models, CD34 (mouse specific) fluorescence was present in the cirrhotic xenograft model but was minimal in the orthotopic and subcutaneous noncirrhotic models. (D) Quantitative analysis of CD34 fluorescence of the human HCC was compared against the corresponding orthotopic cirrhotic PDX, orthotopic noncirrhotic PDX, and subcutaneous noncirrhotic PDX derived from the same human HCC using sum stained intensity and sum stained area value (cellSens Dimension software, Olympus, Tokyo, Japan) (n = 3 for each PDX group). *P < .01; **P < .001. H&E, hematoxylin and eosin; MHC1, major histocompatibility complex 1; hCD34, human-specific CD34; mCD34, mouse-specific CD34; ns, not significant.

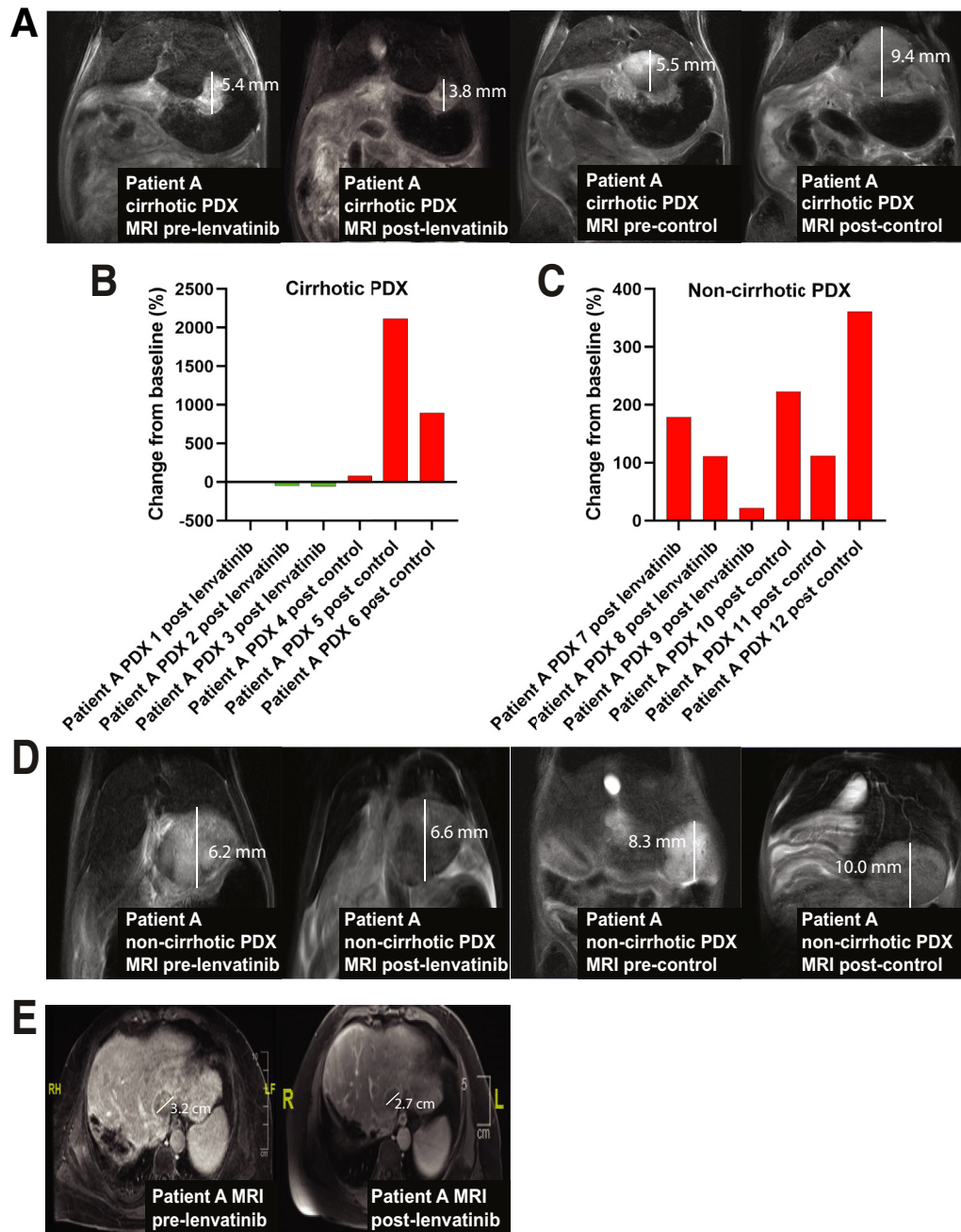
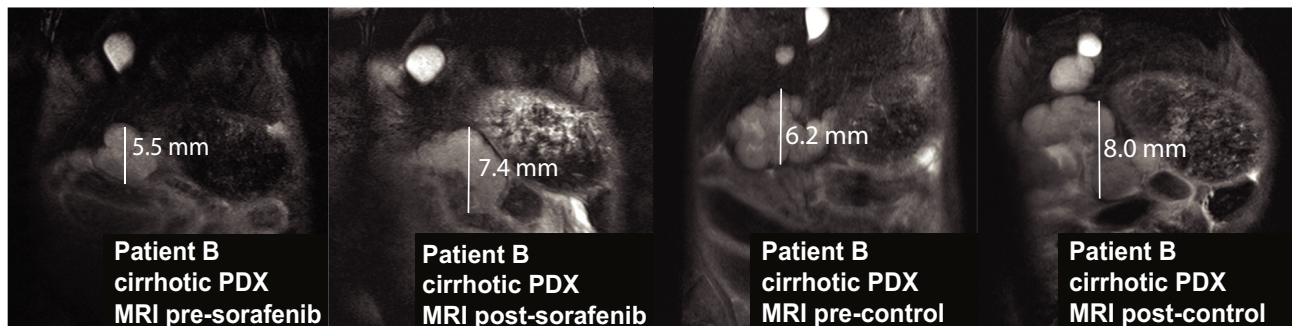


Figure 3. Prediction of clinical response to lenvatinib using the cirrhotic PDX model. (A) Cirrhotic PDX derived from Patient A underwent treatment with 16 days of lenvatinib (30 mg/kg or control for 16 days [n = 3 in each group]). Representative MRIs of cirrhotic PDX derived from Patient A are shown before and immediately after completing treatment with lenvatinib or control. (B) The waterfall plot of cirrhotic PDX tumor response to lenvatinib and control determined by tumor volume on MRI immediately before and at the end of treatment. (C) The waterfall plot of noncirrhotic PDX tumor response to lenvatinib and control determined by tumor volume on MRI immediately before and at the end of treatment. (D) Representative MRIs of noncirrhotic PDX derived from Patient A are shown before and immediately after completing treatment with lenvatinib or control. (E) MRI scan of Patient A before and 2 months after treatment with lenvatinib.

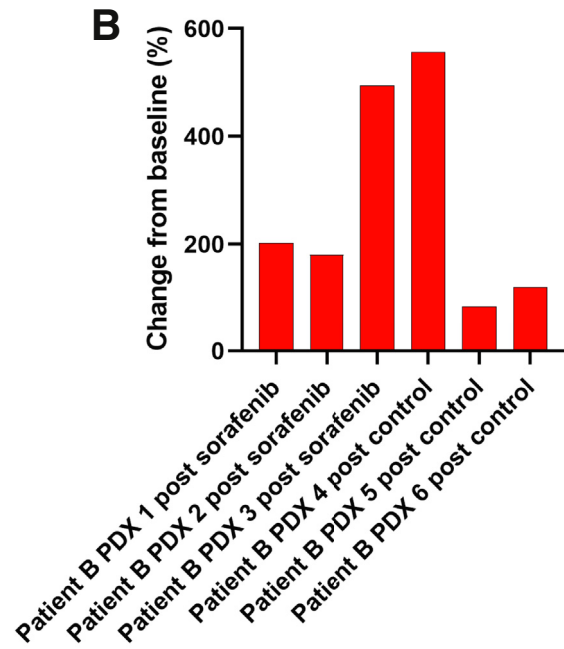
However, limitations of this study include the fact that intratumoral heterogeneity of HCC may result in varying biologic behavior within the cirrhotic PDX model, depending on which portion of the human HCC was sampled for implantation. Second, our study is limited by the small sample

size and these findings should be validated in further studies. Third, the engraftment rate of the cirrhotic model was only 40%, which is an intrinsic limitation of patient-derived animal models for HCC. However, patients with HCC that did not graft into the cirrhotic PDX had more

A



B



C

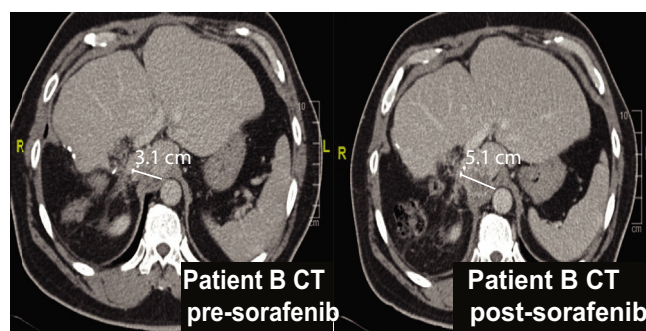


Figure 4. Prediction of clinical nonresponse to sorafenib using the cirrhotic PDX model. (A) Cirrhotic PDX derived from Patient B underwent treatment with 16 days of sorafenib (50 mg/kg for 4 days and then 100 mg/kg for a further 12 days or control for 16 days [$n = 3$ in each group], respectively). Representative MRIs of cirrhotic PDX derived from Patient B are shown before and immediately after completing treatment with sorafenib. (B) The waterfall plot of cirrhotic PDX tumor response to sorafenib and control determined by tumor volume on MRI immediately before and at the end of treatment. (C) Computed tomography scan of Patient B before treatment with sorafenib and repeated 2 months after treatment initiation. CT, computed tomography.

differentiated HCC with a better prognosis than those with HCC that engrafted, with less than 33% developing recurrence.

Conclusions

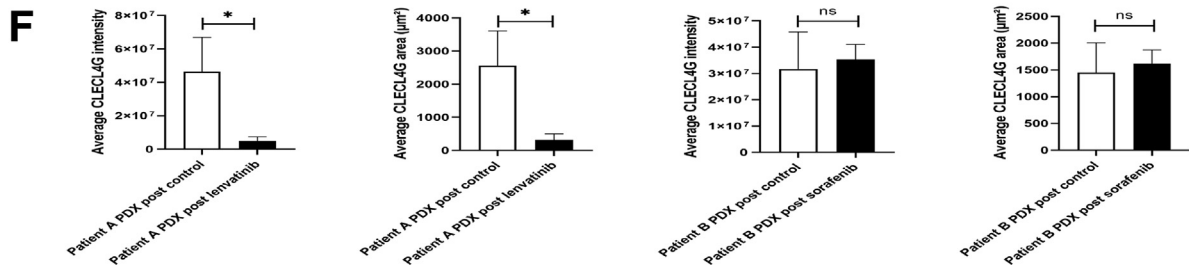
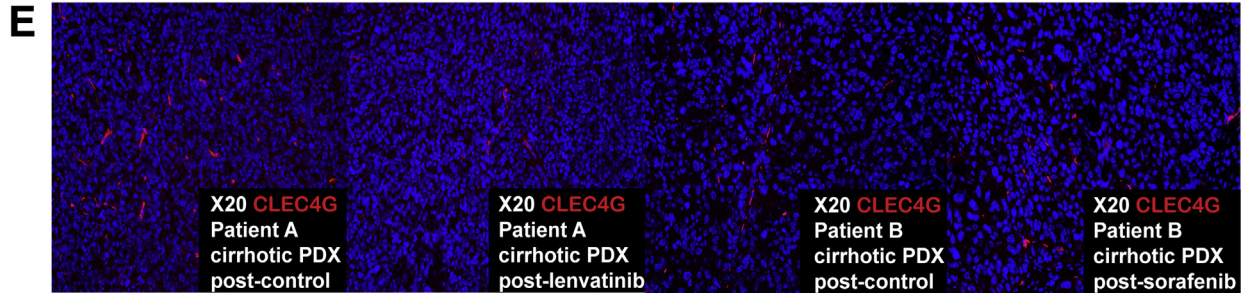
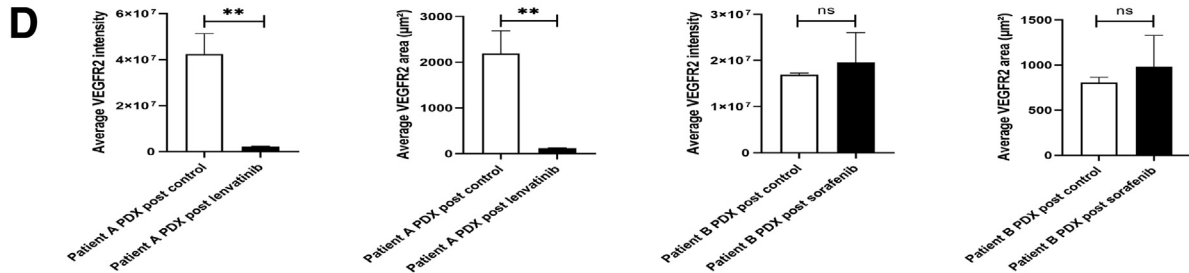
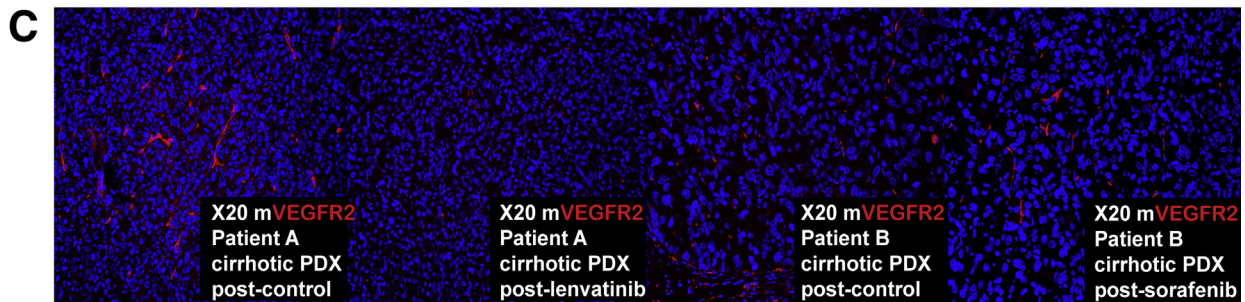
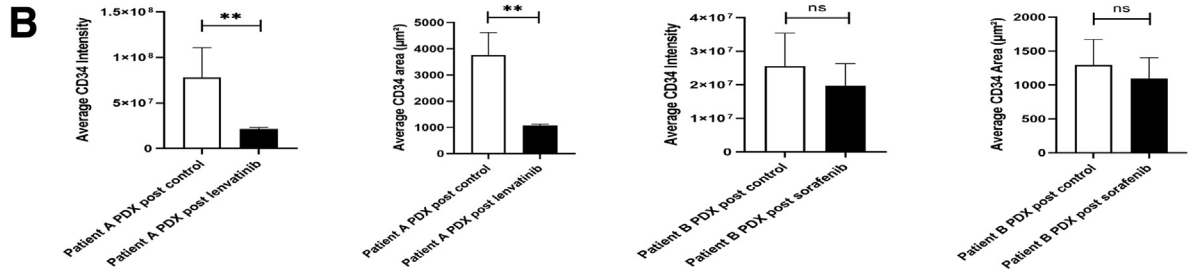
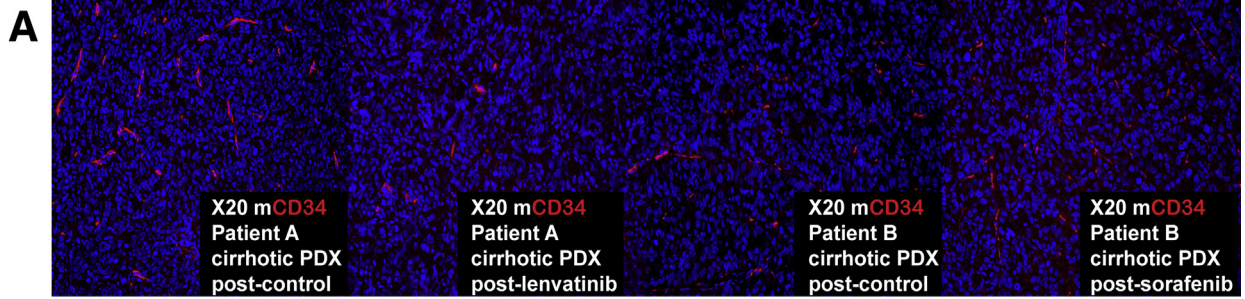
Inhibition of angiogenesis in HCC is a key mode of action of multikinase inhibitors, and current animal models lack the proangiogenic tumor microenvironment to predict tumor response. We demonstrate how the cirrhotic microenvironment allows preferential engraftment of aggressive HCC and prediction of response to multikinase inhibitors by preserving tumor angiogenesis. Our findings, if further validated, may identify patients at high risk for HCC recurrence and allow preemptive drug testing to select efficacious systemic therapy options before HCC recurrence. The

ability to predict the natural biology and personalize therapy using a clinically relevant cirrhotic model holds tremendous implications for treatment of HCC.

Materials and Methods

Animals

We have previously reported an immune-permissive murine model of liver fibrosis using thioacetamide in male NSG NOD.Cg-Prkdc^{scid} Il2rg^{tm1Wjl}/SzJ mice that captures the full clinical picture of structural and functional cirrhosis.¹⁸ The mice were housed in individually ventilated caging systems in groups of 5 (Allentown, NJ) in CeLS Vivarium, Centre for Life Sciences, National University of Singapore. Environmental conditions were regulated to a temperature of 21°C–25°C, humidity of 40%–70%, and a 12:12 light/



dark cycle with lights on at 0700 and off at 1900. The mice were provided with rodent maintenance food (#2918 Teklad Irradiated Global, 18% Protein rodent diet, Envigo, Hackensack, NJ) and bedding from BioCOB. Animals were monitored once daily for health status and no adverse events were observed. Mice with body weight less than 30 g were excluded from the experiment. The mice received care according to the criteria outlined in the Guide for the Care and Use of Laboratory Animals prepared by the National Academy of Sciences³³ and approval for procedures was obtained from the Institutional Animal Care and Use Committee (Protocol no: R17-0888). This study was performed in accordance with the ARRIVE guidelines.

Induction of Cirrhosis

The mice were assigned randomly to thioacetamide and control arms. Thioacetamide (200 mg/L; Sigma-Aldrich, St. Louis, MO) was dissolved in drinking water for administration to NSG mice (starting at age 3 months) for 4 months as previously described.¹⁸ Control mice were fed with plain drinking water.

Creation of Patient-Derived Xenograft

Fresh tumor tissue was obtained from 19 patients who underwent liver resection for HCC. Written informed consent was obtained according to the criteria of the Institutional Review Board of National University Hospital, Singapore (NHG-DSRB Ref: 2011/01580). A portion of the harvested tumor tissue from each patient was processed immediately by direct mincing before being transplanted intrahepatically into the left lobe of 3 NSG cirrhotic mice, and subcutaneously into 3 noncirrhotic NSG mice that were fed with control instead of thioacetamide. In addition to the subcutaneous transplants in noncirrhotic mice mentioned previously, a single PDX line derived from 1 of the previously mentioned 19 patients with HCC was transplanted intrahepatically into the left lobe of 3 noncirrhotic NSG mice and compared against the corresponding cirrhotic orthotopic PDX derived from the same human HCC to test the criticality of cirrhosis on xenograft HCC biology. Each mouse was transplanted with small human HCC tissue fragments of $3 \times 3 \times 3$ mm (containing approximately $2-3 \times 10^6$ cells)

either subcutaneously or intrahepatically. For intrahepatic transplant, the mice were anesthetized with isoflurane, and the livers were located through a small midline incision. The human HCC tissue was suspended in Corning Matrigel Matrix HC (Corning, Cat NO: 354248) before injection into the mice livers. The livers were returned to the abdominal cavity and the incision sites were closed with sutures.

After 1 month, the mice were sacrificed, and their livers were harvested. Tissues from the nonimplanted human HCC, cirrhotic orthotopic xenograft, and noncirrhotic subcutaneous xenograft were formalin-fixed and embedded in paraffin. Hematoxylin and eosin slides of the harvested human HCC and xenograft tissue were reviewed by a liver pathologist. The flow of the study is shown in Figure 1.

Immunofluorescence

To evaluate the immunofluorescence profile of the tumors, 4- μ m-thick tissue sections were stained with antibodies with immunofluorescence for α -fetoprotein (Cell Signaling, Danvers, MA), albumin (MP Biomedicals, Santa Ana, CA), EPCAM (Cell Signaling), CD34 (Abcam for both mouse- and human-specific antibody; Cambridge, UK), E cadherin (Cell Signaling, Cambridge, UK), mouse-specific VEGFR2 (Abcam), human-specific VEGFR2 (R&D Systems, Minneapolis, MN), CLEC4G,³⁴ and vimentin (DAKO, Santa Clara, CA).

Sorafenib and Lenvatinib Administration

Two cirrhotic PDX lines were selected for treatment with lenvatinib (Eisai, Bunkyo-ku, Japan) or sorafenib (Bayer, Leverkusen, Germany). One month after transplantation of human HCC into the liver of mice, MRI of the mice livers was performed before administration of sorafenib/lenvatinib or control (Figure 1). Lenvatinib (Eisai) was dissolved in 3 mmol/L HCl and administered orally to cirrhotic PDX ($n = 3$) derived from a patient with hepatitis C cirrhosis and HCC (Patient A), once daily at a dose of 30 mg/kg for 16 days. This was compared against administration of control (3 mmol/L HCL) against 3 cirrhotic PDX. One member of the study team was assigned to provide either drug or control treatment; another team member was blinded to the treatment provided and performed the outcome assessment.

Figure 5. (See previous page). Response to multikinase inhibitor is associated with reduction in HCC tumor vasculature in the cirrhotic PDX model. (A) Mouse-specific CD34 fluorescence of the cirrhotic PDX tumors derived from Patients A and B was evaluated after treatment with lenvatinib/control and sorafenib/control, respectively ($n = 3$ each group). Representative images are shown. (B) Quantitative analysis of CD34 fluorescence of the cirrhotic PDX tumors derived from Patients A and B was performed using sum stained intensity and sum stained area value (cellSens Dimension software, Olympus, Tokyo, Japan) after treatment with lenvatinib/control and sorafenib/control, respectively ($n = 3$ each group). This demonstrated a significant reduction in average intensity and area of CD34 after treatment with lenvatinib as compared with control, but not with sorafenib as compared with control. (C) Mouse-specific VEGFR2 fluorescence of the cirrhotic PDX tumors derived from Patients A and B was evaluated after treatment with lenvatinib/control and sorafenib/control, respectively ($n = 3$ each group). Representative images are shown. (D) Quantitative analysis of VEGFR2 fluorescence of the cirrhotic PDX tumors derived from Patients A and B was performed using sum stained intensity and sum stained area value after treatment with lenvatinib/control and sorafenib/control, respectively ($n = 3$ each group). (E) CLEC4G fluorescence of the cirrhotic PDX tumors derived from Patients A and B was evaluated after treatment with lenvatinib/control and sorafenib/control, respectively ($n = 3$ each group). Representative images are shown. (F) Quantitative analysis of CLEC4G fluorescence of the cirrhotic PDX tumors derived from Patients A and B was performed using sum stained intensity and sum stained area value after treatment with lenvatinib/control and sorafenib/control, respectively ($n = 3$ each group). * $P < .05$; ** $P < .01$. mCD34, mouse-specific CD34; mVEGFR2, mouse-specific VEGFR2; ns, not significant.

Sorafenib (Bayer) or control (cremophor EL/ethanol) was administered to additional cirrhotic PDX ($n = 3$ in each group) derived from a patient with hepatitis B cirrhosis and HCC (Patient B). Sorafenib was administered orally, once daily at a dose of 50 mg/kg for 4 days and then 100 mg/kg for a further 12 days. Sorafenib was suspended in cremophor EL/95% ethanol (50:50; Sigma Cremophor EL, 95% alcohol).

The mice were sacrificed after 16 days of treatment and the livers were harvested. A repeat MRI was performed immediately before sacrifice. Tumor volumes in 3 dimensions were determined from MRI images using the formula tumor volume = height \times length \times width \times $\pi/6$. Quantitative analysis of immunofluorescence was performed using sum stained intensity and sum stained area (cellSens Dimension software, Olympus, Tokyo, Japan) comparing treatment with multikinase inhibitor versus control. Six random areas for each sample at $\times 20$ magnification were analyzed.

Statistical Analysis

Categorical values between groups were compared using chi-square tests, and continuous variables between groups were analyzed using Student *t* tests and rank sum test. Error bars represent standard error of $n = 3$ biologic samples. A 2-sided *P* value of $< .05$ was considered as a threshold for statistical significance. SPSS version 20.0 (IBM, Armonk, NY) and GraphPad Prism version 6.0 (GraphPad Software, La Jolla, CA) were used to perform statistical analysis.

References

1. Yang JD, Hainaut P, Gores GJ, Amadou A, Plymth A, Roberts LR. A global view of hepatocellular carcinoma: trends, risk, prevention and management. *Nat Rev Gastroenterol Hepatol* 2019;16:589–604.
2. Chayanupatkul M, Omino R, Mittal S, Kramer JR, Richardson P, Thrift AP, El-Serag HB, Kanwal F. Hepatocellular carcinoma in the absence of cirrhosis in patients with chronic hepatitis B virus infection. *J Hepatol* 2017;66:355–362.
3. Hernandez-Gea V, Toffanin S, Friedman SL, Llovet JM. Role of the microenvironment in the pathogenesis and treatment of hepatocellular carcinoma. *Gastroenterology* 2013;144:512–527.
4. Hoshida Y, Villanueva A, Kobayashi M, Peix J, Chiang DY, Camargo A, Gupta S, Moore J, Wrobel MJ, Lerner J, Reich M, Chan JA, Glickman JN, Ikeda K, Hashimoto M, Watanabe G, Daidone MG, Roayaie S, Schwartz M, Thung S, Salvesen HB, Gabriel S, Mazzaferro V, Bruix J, Friedman SL, Kumada H, Llovet JM, Golub TR. Gene expression in fixed tissues and outcome in hepatocellular carcinoma. *N Engl J Med* 2008;359:1995–2004.
5. Pinzani M, Marra F. Cytokine receptors and signaling in hepatic stellate cells. *Semin Liver Dis* 2001;21:397–416.
6. Tu T, Budzinska MA, Maczurek AE, Cheng R, Di Bartolomeo A, Warner FJ, McCaughan GW, McLennan SV, Shackel NA. Novel aspects of the liver microenvironment in hepatocellular carcinoma pathogenesis and development. *Int J Mol Sci* 2014;15:9422–9458.
7. Lee JS, Semela D, Iredale J, Shah VH. Sinusoidal remodeling and angiogenesis: a new function for the liver-specific pericyte? *Hepatology* 2007;45:817–825.
8. Tanigawa N, Lu C, Mitsui T, Miura S. Quantitation of sinusoid-like vessels in hepatocellular carcinoma: its clinical and prognostic significance. *Hepatology* 1997;26:1216–1223.
9. Fang J-H, Xu L, Shang L-R, Pan C-Z, Ding J, Tang Y-Q, Liu H, Liu C-X, Zheng J-L, Zhang Y-J, Zhou Z-G, Xu J, Zheng L, Chen M-S, Zhuang S-M. Vessels That encapsulate tumor clusters (VETC) pattern is a predictor of sorafenib benefit in patients with hepatocellular carcinoma. *Hepatology* 2019;70:824–839.
10. Kudo M, Finn RS, Qin S, Han K-H, Ikeda K, Piscaglia F, Baron A, Park J-W, Han G, Jassem J, Blanc JF, Vogel A, Komov D, Evans TRJ, Lopez C, Dutcus C, Guo M, Saito K, Kraljevic S, Tamai T, Ren M, Cheng A-L. Lenvatinib versus sorafenib in first-line treatment of patients with unresectable hepatocellular carcinoma: a randomised phase 3 non-inferiority trial. *Lancet* 2018;391:1163–1173.
11. Llovet JM, Ricci S, Mazzaferro V, Hilgard P, Gane E, Blanc J-F, de Oliveira AC, Santoro A, Raoul J-L, Forner A, Schwartz M, Porta C, Zeuzem S, Bolondi L, Greten TF, Galle PR, Seitz J-F, Borbath I, Häussinger D, Giannaris T, Shan M, Moscovici M, Voliotis D, Bruix J; SHARP Investigators Study Group. Sorafenib in advanced hepatocellular carcinoma. *N Engl J Med* 2008;359:378–390.
12. Bruix J, Cheng A-L, Meinhardt G, Nakajima K, De Sanctis Y, Llovet J. Prognostic factors and predictors of sorafenib benefit in patients with hepatocellular carcinoma: analysis of two phase III studies. *J Hepatol* 2017;67:999–1008.
13. Gu Q, Zhang B, Sun H, Xu Q, Tan Y, Wang G, Luo Q, Xu W, Yang S, Li J, Fu J, Chen L, Yuan S, Liang G, Ji Q, Chen S-H, Chan C-C, Zhou W, Xu X, Wang H, Fang DD. Genomic characterization of a large panel of patient-derived hepatocellular carcinoma xenograft tumor models for preclinical development. *Oncotarget* 2015;6:20160–20176.
14. Hu B, Li H, Guo W, Sun Y-F, Zhang X, Tang W-G, Yang L-X, Xu Y, Tang X-Y, Ding G-H, Qiu S-J, Zhou J, Li Y-X, Fan J, Yang X-R. Establishment of a hepatocellular carcinoma patient-derived xenograft platform and its application in biomarker identification. *Int J Cancer* 2020;146:1606–1617.
15. Sasaki K, Shindoh J, Margonis GA, Nishioka Y, Andreatos N, Sekine A, Hashimoto M, Pawlik TM. Effect of background liver cirrhosis on outcomes of hepatectomy for hepatocellular carcinoma. *JAMA Surg* 2017;152:e165059.
16. Wörns MA, Weinmann A, Pflingst K, Schulte-Sasse C, Messow C-M, Schulze-Bergkamen H, Teufel A, Schuchmann M, Kanzler S, Düber C, Otto G, Galle PR. Safety and efficacy of sorafenib in patients with advanced hepatocellular carcinoma in consideration of

- concomitant stage of liver cirrhosis. *J Clin Gastroenterol* 2009;43:489–495.
17. Wu Y, Wang J, Zheng X, Chen Y, Huang M, Huang Q, Xiao W, Wei H, Tian Z, Sun R, Sun C. Establishment and preclinical therapy of patient-derived hepatocellular carcinoma xenograft model. *Immunol Lett* 2020;223:33–43.
 18. Muthiah MD, Huang DQ, Zhou L, Jumat NH, Choolani M, Chan JKY, Wee A, Lim SG, Dan Y-Y. A murine model demonstrating reversal of structural and functional correlates of cirrhosis with progenitor cell transplantation. *Sci Rep* 2019;9:1–12.
 19. Finn RS, Qin S, Ikeda M, Galle PR, Ducreux M, Kim T-Y, Kudo M, Breder V, Merle P, Kaseb AO, Li D, Verret W, Xu D-Z, Hernandez S, Liu J, Huang C, Mulla S, Wang Y, Lim HY, Zhu AX, Cheng A-L. IMbrave150 Investigators. Atezolizumab plus bevacizumab in unresectable hepatocellular carcinoma. *N Engl J Med* 2020;382:1894–1905.
 20. Shrum B, Costello P, McDonald W, Howlett C, Donnelly M, McAlister VC. In vitro three dimensional culture of hepatocellular carcinoma to measure prognosis and responsiveness to chemotherapeutic agents. *Hepatobiliary Surg Nutr* 2016;5:204–208.
 21. Marisi G, Cucchetti A, Ulivi P, Canale M, Cabibbo G, Solaini L, Foschi FG, De Matteis S, Ercolani G, Valgiusti M, Frassinetti GL, Scartozzi M, Casadei Gardini A. Ten years of sorafenib in hepatocellular carcinoma: are there any predictive and/or prognostic markers? *World J Gastroenterol* 2018;24:4152–4163.
 22. Tahmasebi Birgani M, Carloni V. Tumor microenvironment, a paradigm in hepatocellular carcinoma progression and therapy. *Int J Mol Sci* 2017;18:405.
 23. Sia D, Alsinet C, Newell P, Villanueva A. VEGF signaling in cancer treatment. *Curr Pharm Des* 2014;20:2834–2842.
 24. Wilhelm SM, Carter C, Tang L, Wilkie D, McNabola A, Rong H, Chen C, Zhang X, Vincent P, McHugh M, Cao Y, Shujath J, Gawlak S, Eveleigh D, Rowley B, Liu L, Adnane L, Lynch M, Auclair D, Taylor I, Gedrich R, Voznesensky A, Riedl B, Post LE, Bollag G, Trail PA. BAY 43-9006 exhibits broad spectrum oral antitumor activity and targets the RAF/MEK/ERK pathway and receptor tyrosine kinases involved in tumor progression and angiogenesis. *Cancer Res* 2004;64:7099–7109.
 25. Llovet JM, Montal R, Sia D, Finn RS. Molecular therapies and precision medicine for hepatocellular carcinoma. *Nat Rev Clin Oncol* 2018;15:599–616.
 26. Choi SYC, Lin D, Gout PW, Collins CC, Xu Y, Wang Y. Lessons from patient-derived xenografts for better in vitro modeling of human cancer. *Adv Drug Deliv Rev* 2014;79–80:222–237.
 27. Reiberger T, Chen Y, Ramjiawan RR, Hato T, Fan C, Samuel R, Roberge S, Huang P, Lauwers GY, Zhu AX, Bardeesy N, Jain RK, Duda DG. An orthotopic mouse model of hepatocellular carcinoma with underlying liver cirrhosis. *Nat Protoc* 2015;10:1264–1274.
 28. Cao G, Li X, Qin C, Li J. Prognostic value of VEGF in hepatocellular carcinoma patients treated with sorafenib: a meta-analysis. *Med Sci Monit* 2015;21:3144–3151.
 29. He S, Hu B, Li C, Lin P, Tang W-G, Sun Y-F, Feng F-Y-M, Guo W, Li J, Xu Y, Yao Q-L, Zhang X, Qiu S-J, Zhou J, Fan J, Li Y-X, Li H, Yang X-R. PDXliver: a database of liver cancer patient derived xenograft mouse models. *BMC Cancer* 2018;18:550.
 30. Yan M, Li H, Zhao F, Zhang L, Ge C, Yao M, Li J. Establishment of NOD/SCID mouse models of human hepatocellular carcinoma via subcutaneous transplantation of histologically intact tumor tissue. *Chin J Cancer Res* 2013;25:289–298.
 31. Tamura S, Kato T, Berho M, Misiakos EP, O'Brien C, Reddy KR, Nery JR, Burke GW, Schiff ER, Miller J, Tzakis AG. Impact of histological grade of hepatocellular carcinoma on the outcome of liver transplantation. *Arch Surg* 2001;136:25–30, discussion 31.
 32. Yip VS, Gomez D, Tan CY, Staettner S, Terlizzo M, Fenwick S, Malik HZ, Ghaneh P, Poston G. Tumor size and differentiation predict survival after liver resection for hepatocellular carcinoma arising from non-cirrhotic and non-fibrotic liver: a case-controlled study. *Int J Surg* 2013;11:1078–1082.
 33. National Research Council (US). Committee for the Update of the Guide for the Care and Use of Laboratory Animals. *Guide for the Care and Use of Laboratory Animals*. 8th ed. 2011 Washington (DC): National Academies Press (US), 2011, Available at: <http://www.ncbi.nlm.nih.gov/books/NBK54050/>. Accessed May 25, 2020.
 34. Zuo Y, Ren S, Wang M, Liu B, Yang J, Kuai X, Lin C, Zhao D, Tang L, He F. Novel roles of liver sinusoidal endothelial cell lectin in colon carcinoma cell adhesion, migration and in-vivo metastasis to the liver. *Gut* 2013;62:1169–1178.

Received July 28, 2020. Accepted December 14, 2020.

Correspondence

Address correspondence to: Yock Young Dan, MBBS, PhD, University Medicine Cluster, National University Health System, 1E, Kent Ridge Road, NUHS Tower Block Level 10, Singapore 119228. e-mail: mdcdyy@nus.edu.sg; fax: 6567751518.

Acknowledgments

Daniel Huang and Yock Young Dan designed the study. Daniel Huang, Zhou Lei, Tan Wan Xin, Gwyneth Soon, and Yi Ting Lim acquired the data. Daniel Huang analyzed the data. Daniel Huang, Mark Muthiah, Gwyneth Soon, and Yock Young Dan drafted the manuscript. All authors interpreted the data and reviewed/revised the manuscript. Yock Young Dan and Daniel Huang were responsible for study concept and study supervision. All authors approved the author list, had access to the study data, and reviewed and approved the final manuscript.

CRedit Authorship Contributions

Daniel Q. Huang (Conceptualization: Lead; Data curation: Lead; Formal analysis: Lead; Investigation: Lead; Methodology: Lead; Resources: Lead; Validation: Lead; Writing – original draft: Lead)

Mark D. Muthiah (Writing – original draft: Supporting; Writing – review & editing: Supporting)

Lei Zhou (Data curation: Supporting; Writing – review & editing: Supporting)

Halisah Jumat (Data curation: Supporting; Writing – review & editing: Supporting)

Wan Xin Tan (Data curation: Supporting; Writing – review & editing: Supporting)

Guan Huei Lee (Data curation: Supporting; Writing – review & editing: Supporting)

Seng Gee Lim (Data curation: Supporting; Writing – review & editing: Supporting)

Alfred Kow (Data curation: Supporting; Writing – review & editing: Supporting)

Glenn Bonney (Data curation: Supporting; Writing – review & editing: Supporting)

Iyer Shridhar (Data curation: Supporting; Writing – review & editing: Supporting)

Yi Ting Lim (Conceptualization: Supporting; Data curation: Supporting; Investigation: Supporting; Writing – review & editing: Supporting)

Aileen Wee (Data curation: Supporting; Writing – original draft: Supporting)
Yin Huei Pang (Data curation: Supporting; Writing – original draft: Supporting)

Gwyneth Soon (Data curation: Supporting; Writing – original draft: Supporting; Writing – review & editing: Supporting)

Pierce Chow (Data curation: Supporting; Writing – review & editing: Supporting)

Yock-Young Dan, MBBS, PhD (Conceptualization: Supporting; Data curation: Supporting; Formal analysis: Supporting; Funding acquisition: Lead; Investigation: Supporting; Methodology: Supporting; Project administration: Lead; Resources: Lead; Supervision: Lead; Writing – original draft: Supporting; Writing – review & editing: Supporting)

Conflicts of interest

These authors disclose the following: Lim Seng Gee advises and received grants from Gilead, Abbott, and Roche; advises AbbVie, Springbank, Kaleido

Biosciences, and Arbutus; and received grants from Fibronostics and Merck. Dan Yock Young serves as a consultant for Novartis, Boehringer Ingelheim, Gilead, and AbbVie. The other authors disclose no conflicts.

Funding

Daniel Q. Huang is supported by Exxon Mobil-NUS Research Fellowship for Clinicians and Singapore Ministry of Health's National Medical Research Council under its NMRC Research Training Fellowship. Mark D. Muthiah is supported by Singapore Ministry of Health's National Medical Research Council under its NMRC Research Training Fellowship MOH-000193. Guan Huei Lee is supported by Singapore Ministry of Health's National Medical Research Council Clinician Scientist Award (NMRC/ CSA-INV/0024/2017). Pierce Chow is supported by Singapore Ministry of Health's National Medical Research Council Clinician Scientist Award (NMRC/CSA-SI/0018/2017). Yock Young Dan receives funding support from A*Star BMRC (H17/01/a0/003).